ELSEVIER

International Journal of Mass Spectrometry 185/186/187 (1999) 231–240

The unimolecular chemistry of protonated hydroxylamine

Elisabeth Leere Øiestad, Einar Uggerud*

Department of Chemistry, University of Oslo, P.O. Box 1033 Blindern, N-0315 Oslo, Norway

Received 28 May 1998; accepted 6 July 1998

Abstract

The unimolecular chemistry of protonated hydroxylamine has been investigated using mass spectrometric and ab initio methods. Calculation of the proton affinity shows that the nitrogen atom is the most basic site. There is an activation barrier of 211 kJ mol^{-1} for the isomerization to the structure corresponding to protonation on oxygen. Thorough studies of the potential energy surface by ab initio methods correlate well with the observed peaks in the mass-analyzed ion kinetic energy (MIKE) spectrum. ^{15}N labelling has been used to identify fragmentation products unambiguously. In contrast to several isoelectronic systems, loss of H_2 is not a major process in the MIKE-spectrum. The importance of spin change, as has recently been seen for other protonated systems, becomes evident in this study. The theoretical calculations show that the main process, loss of NH, can only be explained by a cross-over from the singlet to the triplet surface. (Int J Mass Spectrom 185/186/187 (1999) 231–240) © 1999 Elsevier Science B.V.

Keywords: Unimolecular chemistry; Ab initio quantum chemistry; Spin-orbit coupling; Proton affinity; Mass spectrometry

---

1. Introduction

The unimolecular chemistry of small protonated molecules consisting of two main group atoms (X,Y = C,N,O,F,S) and a number of hydrogens has been the focus of several laboratories, including ours, for some time [1–12]. The typical reactions are $H^{\cdot}$ -loss, H_2 loss, and cleavage of the X–Y bond (Scheme 1).

$$\begin{array}{ll} & \nearrow XYH_{n-1}^{+\cdot} + H^{\cdot} \\ XYH_n^+ & \rightarrow XYH_{n-2}^{+} + H_2 \\ & \searrow XH_{n-m}^{+} \ \ + YH_m \end{array}$$

Scheme 1.

Thorough quantum chemical surveys of some of these protonated molecules have shown that such small systems [8, 13, 14] may have surprisingly complicated potential energy surfaces.

Recent studies of the protonated forms of formaldehyde [15–18], CH_2OH^+, methylene imine [14, 15], $CH_2NH_2^+$, diazene [14], $NHNH_2^+$, thioformaldehyde [15], CH_2SH^+, hydrazine [19], $NH_2NH_3^+$, and ethene [20], $CH_2CH_3^+$, show the ongoing interest in the field. The topics for these studies were the mechanisms of the different reaction pathways, including detailed reaction dynamics and energy partitioning. The characteristic H_2-elimination reaction has been studied in great detail, and in most cases a large fraction of the reverse energy is liberated as translational energy.

Protonated methylamine [7, 11], $CH_3NH_3^+$, reacts in accordance with Scheme 1, though with little NH_3 elimination. The H_2 elimination is associated with a

---

* Corresponding author. E-mail: einar.uggerud@kjemi.uio.no

Dedicated to Professor Michael T. Bowers on the occasion of his 60th birthday.

1387-3806/99/$20.00 © 1999 Elsevier Science B.V. All rights reserved
PII S1387-3806(98)14082-4

large translational energy release, $T_{0.5} = 1.75$ eV, measured at half height. Upon exchange of the nitrogen containing group with the isoelectronic groups containing oxygen, sulphur, or fluoride, the same reactions are observed [7], with loss of HF dominating the reaction of CH_3FH^+, and loss of H_2 dominating the unimolecular reactivity of $CH_3OH_2^+$ and $CH_3SH_2^+$. Exchange of the methyl group with the more electronegative amino group gives protonated hydrazine [19], $NH_2NH_3^+$. In a previous article we showed that the dominating reactions of this species are loss of $H^{\cdot}$ and H_2, in accordance with quantum chemical calculations. In this case, direct heterolytic bond scission is not observed as a reaction on the ground state singlet surface. Instead, a relatively weak signal due to loss of NH is observed, most probably the result of a cross-over to the triplet surface

$$NH_2NH_3^+(\text{singlet}) \rightarrow NH_4^+ + NH(\text{triplet}) \qquad (1)$$

Exchanging the CH_3 group of $CH_3NH_3^+$ with the even more electronegative OH group gives the isoelectronic ion, protonated hydroxylamine NH_3OH^+(**1**) that is the subject of this study. To the best of our knowledge, no detailed study of the unimolecular chemistry of protonated hydroxylamine has previously been reported in the literature.

2. Experimental

The mass-analyzed ion kinetic energy (MIKE) spectra were obtained using a four-sector mass spectrometer (JMS-HX/HX110A, Jeol Ltd., Japan) with EBEB (E = electric sector, B = magnetic sector) geometry (acceleration voltage, $V_0 = 10$ kV). Ions were selected with the first two sectors, and decomposition in the third field-free region was recorded by scanning the second E sector (MIKE scan [21]) of the instrument. Intermediate energy defining slits were set narrow to obtain the highest possible energy resolution, which for this instrument, is better than 0.1%.

Collisionally-induced decomposition (CID) spectra were recorded using the MIKE scan technique with helium gas in the collision cell of the third field-free region of the instrument at 10% transmission of the parent ion. Hydroxylamine in the form of hydroxylammonium chloride (MERCK, KGaA, Darmstadt, Germany; >99% pure) was introduced into a combined electron impact/chemical ionisation source by a direct inlet probe. Protonated hydroxylamine was generated by chemical ionisation with hydrogen as reagent gas. A comparative experiment with ^{15}N isotope labelled hydroxylamine (CDN isotopes, Pointe-Claire, Quebec, Canada; 99% pure) was performed on a VG Prospec-Q (Micromass Ltd., Manchester U.K.) instrument, also employing the MIKE technique to identify fragmentation products unambiguously.

3. Theoretical methods

Quantum chemical calculations were carried out using the program systems GAUSSIAN 94 [22] and DALTON [23]. The GAUSSIAN program was used for all calculations except for the calculation of spin-orbit coupling at structure **TS2/11**, for which the DALTON program was used. The methods used were Hartree–Fock (HF) [24] and Møller–Plesset [25] perturbation theory to the second order (MP2) with a 6-31G** basis set. All stationary points found on the potential energy surface were characterised by complete optimisation of the molecular geometry for both methods of calculation. Harmonic frequencies were obtained from the diagonalized mass-weighted Cartesian force constant matrix, calculated from the analytical second derivatives of the total energy (the Hessian). The zero point vibrational energies (zpve) calculated from the obtained harmonic frequencies at the MP2/6-31G** level of theory were scaled by a factor [26] of 0.9608 and included in the relative energies. The results are presented in Table 1 and geometrical parameters from the MP2/6-31G** calculations are depicted in Fig. 1. Intrinsic reaction coordinate calculations were used to connect the transition structures with the correct reactant and products. The proton affinity corresponding to protonation on either nitrogen or oxygen was calculated by the G2 method [27].

Table 1
Energies from ab initio calculations[a]

Structure	HF/6-31G(d,p) Electronic energy (Hartrees)	MP2/6-31G(d,p) Electronic energy (Hartrees)	E^{b}_{zpv} kJ (kJ mol^{-1})	Exp[c] $\Delta H^{0}f$,298 (kJ mol^{-1})
1 NH_3OH^+	−131.32411	−131.68547	140.942	676
2 $NH_2OH_2^+$	−131.28470	−131.64215	136.165	
3 $NH_4^+ \cdots O$				
4 NH_4^+	−56.54553	−56.73368	128.390	630
5 O	−74.65660	−74.76995		439
6 $NHOH^+$	−130.05015	−130.38566	72.803	
7 H_2	−1.13113	−1.15766	26.493	0
8 ONH_2^+	−130.07189	−130.41628	72.505	973
9 NH_3	−56.19554	−56.38322	89.456	−46
10 OH^+	−74.83693	−74.95464	18.673	(1666)
11 $NH \cdots H_3O^+$	−131.20762	−131.53320	108.199	
12 ^1NH	−54.85390	−54.97529	19.819	628
13 H_3O^+	−76.31032	−76.50611	89.013	581
14 NH_2^+	−55.13508	−55.25827	47.116	1390
15 H_2O	−76.02362	−76.21979	55.188	−242
16 $NH_2OH^{+\cdot}$	−130.69855	−131.03119	102.830	(923)
17 $H^{\cdot}$	−0.49823			218
18 $NH_3O^{+\cdot}$	−130.68479	−130.99552	102.698	
19 $NHOH_2^{+\cdot}$	−130.65482	−130.97424	98.380	
20 $NH_3^{+\cdot}$	−55.88489	−56.02881	85.437	934
21 $OH^{\cdot}$	−75.38833	−75.53209	22.078	39
22 $NH_2.$	−55.56482	−55.70996	49.802	189
23 $H_2O^{+\cdot}$	−75.62826	−75.77424	48.803	976
24 $^3NH_2OH_2^+$	−131.27194	−131.58613	120.285	
25 $^3NH \cdots H_3O^+$	−131.30936	−131.61479	116.028	
26 ^3NH	−54.96264	−55.06794	19.585	377
TS1/2	−131.21662	−131.59809	122.153	
TS1/3	−131.16370	−131.49438	124.708	
TS1/6+7	−131.15042	−131.52341	106.737	
TS′1/6+7	−131.14029	−131.51384	110.597	
TS1/8+7	−131.04973	−131.43338	111.153	
TS2/8+7	−131.11958	−131.50751	111.926	
TS2/11	−131.20514	−131.53145	110.800	
TS24/25	−131.27191	−131.57611	117.367	

[a] All species are in their singlet spin states, unless otherwise given.
[b] 0.9608 · E_{zpv}[MP2/6-31(d,p)].
[c] See text for references.

4. Thermochemistry and proton affinity

The proton affinity, PA, of hydroxylamine was determined by the G2 method to be 817 kJ mol^{-1} for protonation on nitrogen and 711 kJ mol^{-1} for protonation on oxygen. This is in good agreement with the G1 values of Angelelli et al. [28] of 812 kJ mol^{-1} and 701 kJ mol^{-1}, respectively. The theoretical value found by Angelelli et al. is in excellent agreement with their own experimental value of 812 kJ mol^{-1} determined by the bracketing method. Earlier theoretical calculations by Del Bene et al. [29] with the MP4SDQ/4-31G*//6-31G** wave function give values for the proton affinities of 835 kJ mol^{-1} for nitrogen and 734 kJ mol^{-1} for oxygen. Thermochemical data were taken from the literature [30, 31], and are given in the last column of Table 1. The enthalpies of formation of O, OH^+, NH, and NH_2^+ in their singlet states were obtained by adding the known singlet–triplet energy differences [30, 32] to the corre-

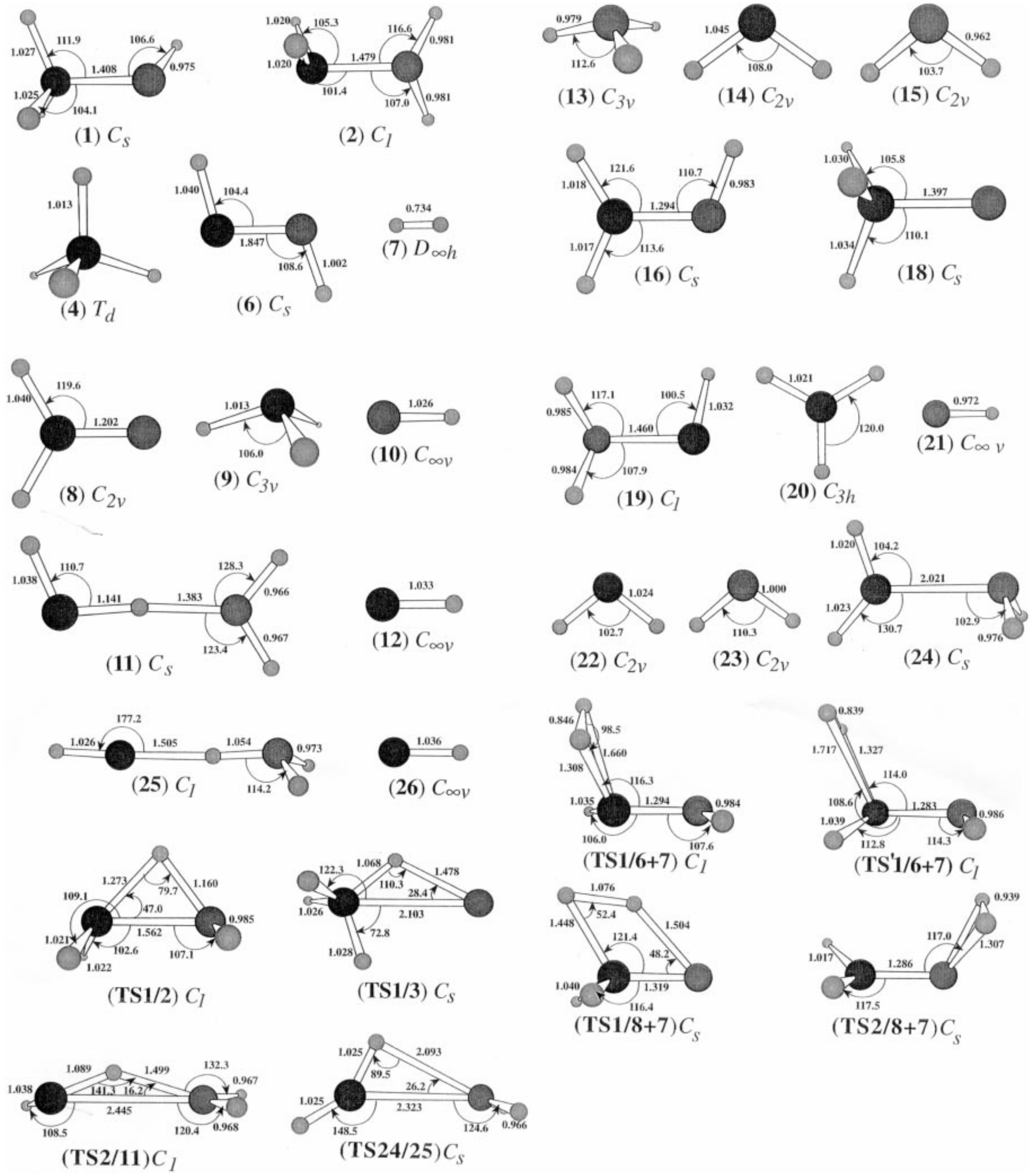

Fig. 1. Geometrical structures of reactants, transition structures, and intermediates of the $[H_2NOH]H^+$ system computed with MP2/6-31G(d,p). The nitrogen atom is marked by a darker grey shade and the oxygen atom by a lighter grey shade. Bond distances are given in angstroms and angles in degrees.

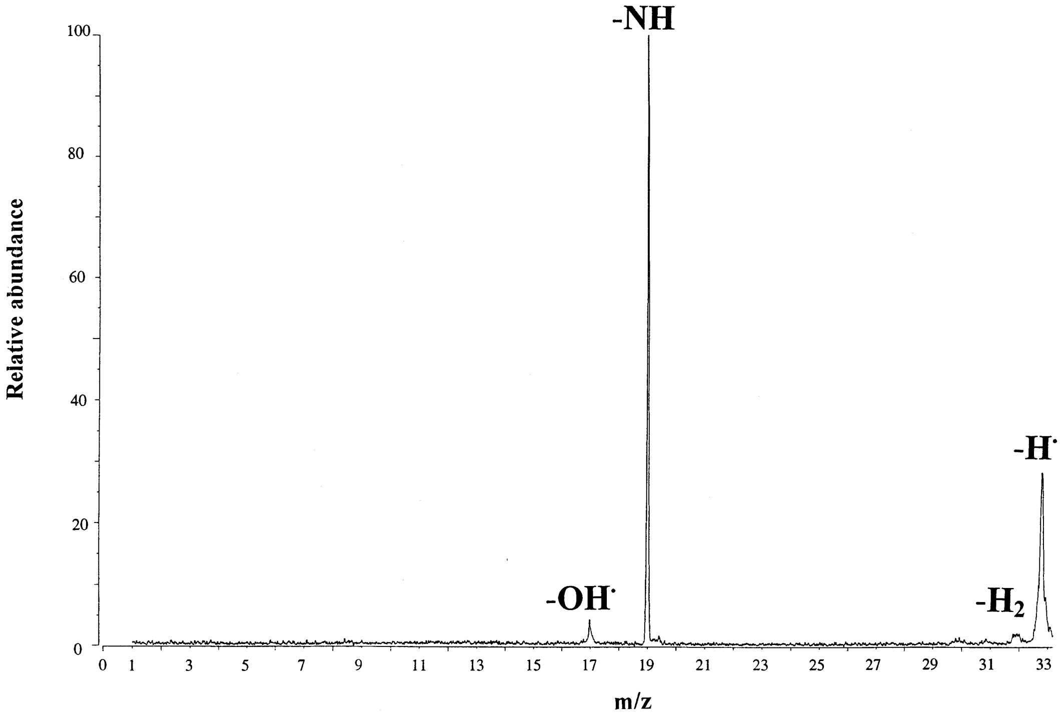

Fig. 2. MIKE spectrum of protonated hydroxylamine ($m/z = 34$). Neutral losses are indicated.

sponding enthalpies of the ground state triplet species. It was found that the MP2/6-31G(d,p) calculations of relative energies are in reasonably good agreement with relative experimental enthalpies (where available).

5. Results and discussion

The main peaks in the MIKE spectrum of protonated hydroxylamine (m/z 34), Fig. 2, are m/z 19 and 33, corresponding to loss of NH and $H^{\cdot}$. A weak signal for m/z 17 (loss of $OH^{\cdot}$) and a signal close to the detection limit for m/z 32 (loss of H_2) are also observed. This assignment of the MIKE spectrum was confirmed in an experiment with ^{15}N labelled hydroxylamine.

Theoretical calculations show that crossing the 211 kJ mol^{-1} barrier for isomerization from NH_3OH^+(**1**) to $NH_2OH_2^+$ (**2**), reaction (2), is the lowest energy process. Reactions from both isomers are therefore possible and total scrambling of the hydrogen atoms must be assumed

$$NH_3OH^+(\mathbf{1}) \rightleftarrows NH_2OH_2^+(\mathbf{2}) \tag{2}$$

Our CID spectrum (not shown here) of $[NH_2OH]H^+$ showed evidence for both isomers, with peaks corresponding to NH_2^+ (m/z 16, relative intensity 30%) and OH^+ (m/z 17, relative intensity 75%) dominating in the range between m/z 14–19. By using less acidic proton donors, Brönstrup et al. [33] have been able to show that protonation on the nitrogen is preferred.

Fig. 3 shows the relative energies for all possible direct bond scissions. There are, in principle, four different ways to lose $H^{\cdot}$ of which reaction (3) and (6) give identical products. All reactions turn out to proceed without reverse activation energy. The lowest energy paths are reaction (3) and (6) at 372 kJ mol^{-1}

$$NH_3OH^+(\mathbf{1}) \rightarrow NH_2OH^{+\cdot}(\mathbf{16}) + H^{\cdot}(\mathbf{17}) \tag{3}$$

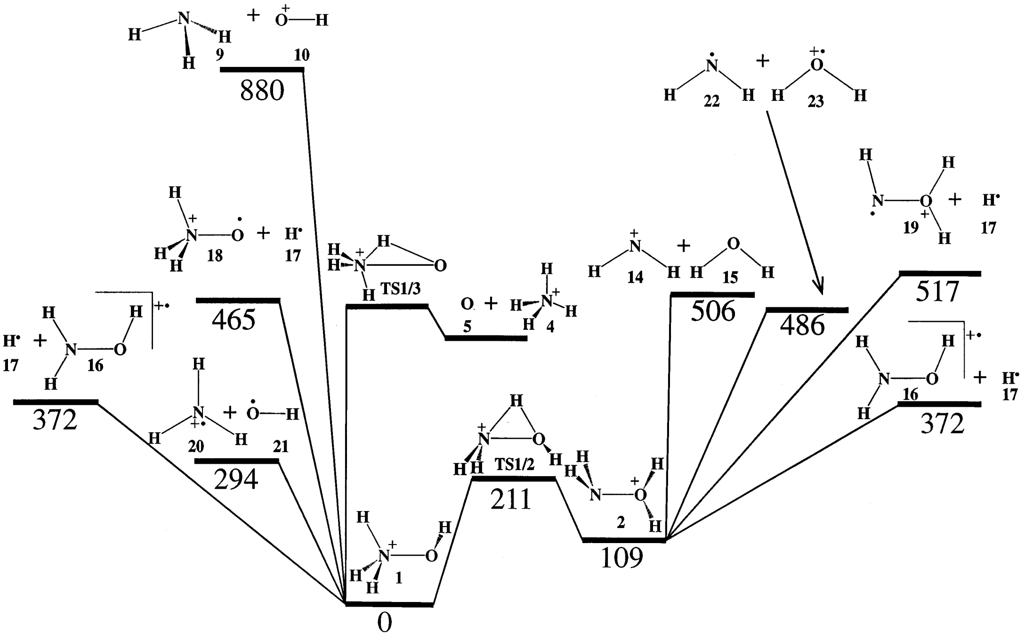

Fig. 3. MP2/6-31G(d,p) potential energy diagram depicting bond breaking processes in the singlet $[H_2NOH]\ H^+$ system. Relative energies indicated are in kJ mol^{-1} and include zpve corrections.

$$NH_3OH^+(\mathbf{1}) + NH_3O^{+\cdot}(\mathbf{18}) + H^{\cdot}(\mathbf{17}) \quad (4)$$

$$NH_2OH_2^+(\mathbf{2}) \rightarrow NHOH_2^{+\cdot}(\mathbf{19}) + H^{\cdot}(\mathbf{17}) \quad (5)$$

$$NH_2OH_2^+(\mathbf{2}) \rightarrow NH_2OH^{+\cdot}(\mathbf{16}) + H^{\cdot}(\mathbf{17}) \quad (6)$$

The only species that can account for the presence of a peak at m/z 19 is H_3O^+ and the ^{15}N labelling experiment confirmed this assignment. This ion can be reached by the low energy isomerization of NH_3OH^+(**1**) to $NH_2OH_2^+$(**2**) and subsequent loss of NH(**12**) via the intermediate complex $NH \cdots H_3O^+$(**11**) (Fig. 4)

$$NH_2OH_2^+(\mathbf{2}) \rightarrow NH \cdots H_3O^+(\mathbf{11})$$
$$\rightarrow NH(\mathbf{12}) + H_3O^+(\mathbf{13}) \quad (7)$$

Energetic considerations indicate that this reaction cannot be the major source of formation of H_3O^+. Although **TS2/11** at 374 kJ mol^{-1} is accessible, the final products are at 504 kJ mol^{-1}. When we compare this with the competing $H^{\cdot}$ loss [reactions (3) and (6)], formation of H_3O^+ as the major reaction cannot be justified from this mechanism.

The importance of spin change in reactions of heavy elements (e.g. in transition metal chemistry) is well known. However recent reports [19, 34–38] demonstrate that this phenomenon is also operative in given cases where the molecular system is composed of first and second row elements. For example, studies of the "spin-forbidden" proton transfer reaction between F^- and ^{1}HNO by Janaway et al. [36] and the "spin-forbidden" unimolecular decay of the methoxy cation by Aschi et al. [37], make it evident that a revision of the strategy of only looking at the singlet surface is necessary. The ground state of the NH molecule is a triplet state. In analogy with the isoelectronic system [19], $NH_2NH_3^+$, we therefore suggest that a cross-over to the triplet surface provides the explanation of the fact that H_3O^+ dominates the MIKE spectrum.

Fig. 4 gives a comparison between the pathways from $NH_2OH_2^+$(**2**) to NH + H_3O^+ on the singlet and triplet surfaces. The triplet route (marked with a dotted line) is lower in energy than the one on the singlet surface (marked with a solid line). It turns out

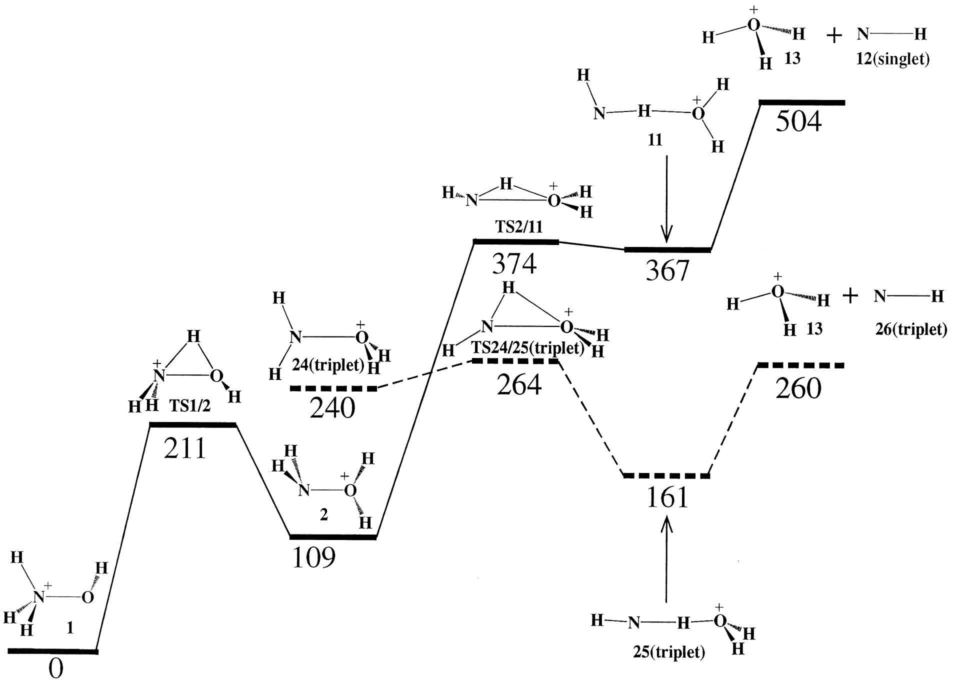

Fig. 4. MP2/6-31G(d,p) potential energy diagram for the route to loss of NH in the $[H_2NOH]\ H^+$ system. The solid line indicates the reaction on the singlet surface, while the dotted line indicates the reaction on the triplet surface. Relative energies indicated are in kJ mol^{-1} and include zpve corrections.

to be the lowest energy product-forming process. Singlet to triplet transitions are driven by spin-orbit coupling [38] that can be calculated using response theory. To check for a substantial spin-orbit coupling in this system, calculation of the spin–orbit coupling at the geometry of **TS2/11** was done with the DALTON [23] program. This gave a total magnitude of 73 cm^{-1} in strong support of the proposed cross-over mechanism.

It is realized that this approach is rather rudimentary. More sophisticated schemes for calculation of accurately defined minimum energy crossing points have been presented [39]. For the present purpose we believe that the estimate given here is realistic.

Fig. 5 shows the calculated pathways for elimination of H_2. Formally, the remaining fragment after loss of H_2 will be protonated nitroxsyl. The theoretical calculations show that the structure protonated on nitrogen, NH_2O^+(**8**), is more stable than the one protonated on oxygen, $NHOH^+$(**6**), by approximately 82 kJ mol^{-1}, agreement with Schröder et al. [13]. Looking at the transition structures, however, the 1,2 H_2 elimination from NH_3OH^+(**1**), reaction (8), is more energy demanding than the 1,1 elimination, reaction (9). There are two different transition structures **TS1/6+7** and **TS′1/6+7** connecting NH_3OH^+(**1**), and $NHOH^+$(**6**). In the first case, the hydrogens in the $NHOH^+$ framework are anti-periplanar in the transition structure, while in the latter they are syn-periplanar. In both cases the distance between the two departing hydrogens is small. As can be seen from Fig. 1, the bond distances in the H_2 moieties are close to the equilibrium bond length of molecular hydrogen

$$NH_3OH^+(\mathbf{1}) \rightarrow NH_2O^+(\mathbf{8}) + H_2(\mathbf{7}) \qquad (8)$$

$$NH_3OH^+(\mathbf{1}) \rightarrow NHOH^+(\mathbf{6}) + H_2(\mathbf{7}) \qquad (9)$$

$$NH_2OH_2^+(\mathbf{2}) \rightarrow NH_2O^+(\mathbf{8}) + H_2(\mathbf{7}) \qquad (10)$$

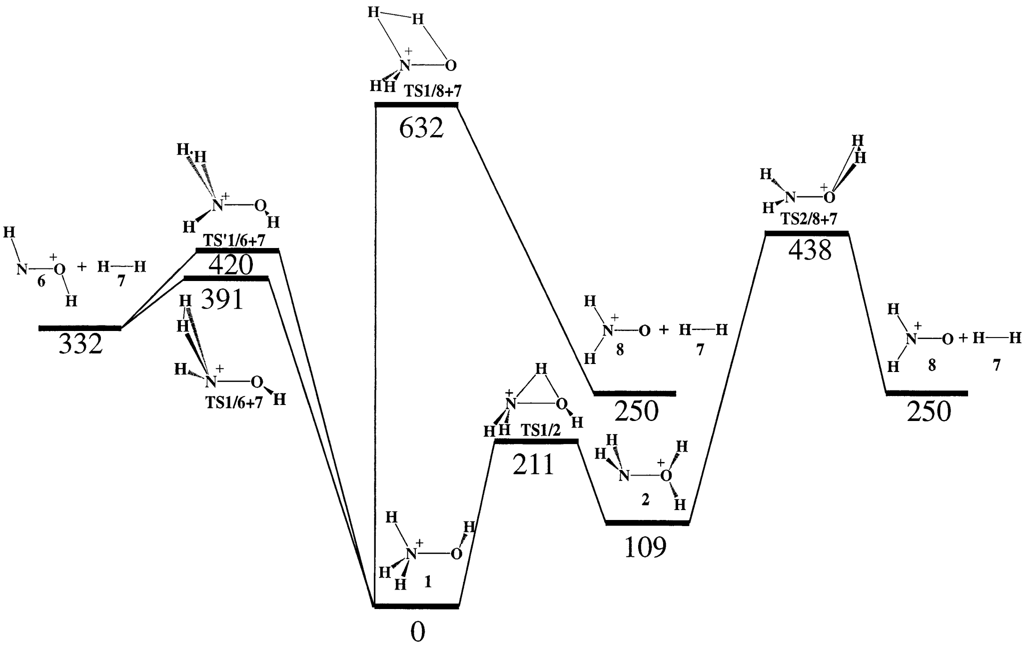

Fig. 5. MP2/6-31G(d,p) potential energy diagram showing pathways for H_2 elimination from the $[H_2NOH]\ H^+$ system. Relative energies indicated are in kJ mol^{-1} and include zpve corrections.

The 1,1 elimination from the $NH_2OH_2^+$(**2**) isomer, reaction (10), has been found to be slightly higher in energy than the 1,1 elimination from NH_3OH^+(**1**). No transition structure corresponding to 1,2 elimination from $NH_2OH_2^+$(**2**) was found. The results of these calculations are in agreement with the very small peak for H_2 loss in the MIKE spectrum.

As shown in Scheme 1, a usual reaction pathway for protonated molecules of the type XYH_n^+ (X,Y = C,N,O,S,F) is heterolytic cleavage of the bond between the two main group atoms. The study of protonated hydrazine [19], $NH_2NH_3^+$, showed that in some cases homolytic bond scission have comparable energetic requirements. For the *m/z* 17 peak in Fig. 2 this means that two possible pathways exist, either heterolytic (11) or homolytic (12) bond scissions

$$NH_3OH^+(\mathbf{1}) \rightarrow NH_3(\mathbf{9}) + OH^+(\mathbf{10})(m/z = 17) \tag{11}$$

$$NH_3OH^+(\mathbf{1}) \rightarrow NH_3^{+\cdot}(\mathbf{20})(m/z = 17) + OH^{\cdot}(\mathbf{21}) \tag{12}$$

The theoretical calculations, Fig. 3, proved the heterolytic bond scission to be very energy demanding, even when we take into account the possibility that OH^+ may be formed in its ground ${}^3\Sigma^-$ state. The triplet is approximately 300 kJ mol^{-1} lower in energy than the singlet depicted in Fig. 3. Homolytic bond scission, on the other hand, turned out to be a low energy process, thus ruling in favour of this being the observed pathway. To avoid any ambiguity, experiments with ^{15}N isotope labelled hydroxylamine were performed. The shift in mass from *m/z* 17 to *m/z* 18 showed that the product ion is indeed $NH_3^{+\cdot}$ (**20**).

The relative peak height of *m/z* 17 (loss of $OH^{\cdot}$) compared to *m/z* 33 (loss of $H^{\cdot}$) appears not to be well reproduced by the calculations, even if we take into account that there are more pathways leading to loss of $H^{\cdot}$. Because reaction (12) is about 80 kJ mol^{-1} lower in energy than reaction (3) and (6) one would expect this to be more prominent. A possible explanation could be that the quartet states for the radical cations remaining after $H^{\cdot}$ loss are lower in energy than the doublet states. Calculations of the quartet states of the species (**16**), (**18**), and (**19**) did, however, rule this out. It also appears that the $H^{\cdot}$ loss peak is too big in comparison with the peak for NH loss (Fig. 2). This indicates that the inconsistency arises from the instrument's discrimination against lower mass ions in the MIKE scan.

Neither heterolytic nor homolytic bond scissions from the $NH_2OH_2^+(\mathbf{2})$ isomer [reaction (13) and (14)] were observed experimentally. As can be seen from Fig. 3, these reactions are approximately 200 kJ mol^{-1} more energy demanding than the homolytic bond scission from the NH_3OH^+ isomer

$$NH_2OH_2^+(\mathbf{2}) \rightarrow NH_2^+(\mathbf{14}) + H_2O(\mathbf{15}) \qquad (13)$$

$$NH_2OH_2^+(\mathbf{2}) \rightarrow NH_2^{\cdot}(\mathbf{22}) + H_2O^{+\cdot}(\mathbf{23}) \qquad (14)$$

The transition structure **TS1/3** at 486 kJ mol^{-1} has the characteristics of a route to NH_4^+, and correspondingly, this high-energy pathway was not observed in the spectrum. Because of convergence problems we were not able to find a stable minimum for the very loosely bounded intermediate complex, $NH_4^+ \cdots O$

$$NH_3OH^+(\mathbf{1}) \rightarrow NH_4^+ \cdots O(\mathbf{3}) \rightarrow NH_4^+(\mathbf{4}) + O(\mathbf{5}) \qquad (15)$$

6. Conclusion

The unimolecular chemistry of protonated hydroxylamine has been investigated both experimentally and theoretically. The dominating processes are loss of $H^{\cdot}$ and NH. Some loss of $OH^{\cdot}$ and H_2 are also observed. The theoretical calculations show that the loss of NH can be explained by cross-over from the singlet to triplet potential energy surface to yield $^3NH + H_3O^+$. This is supported by recent studies that point out the need to acknowledge the importance of spin change even for small systems. Comparison of $OHNH_3^+$ with the isoelectronic systems $CH_3NH_3^+$ and $NH_2NH_3^+$, shows that the inclusion of more electronegative X groups in XNH_3^+ shifts the observed reaction pathways away from heterolytic bond scission and H_2 elimination over to homolytic bond scission and reactions on the triplet surface.

Acknowledgements

The authors wish to thank VISTA (the Norwegian Academy for Science and Letters, and Statoil) for financial support and NFR (the Norwegian Research Council) for computer time. We thank Dr. Kim Norrman and Allan Petterson (Copenhagen), Åse Marit Leere Øiestad and Hilde Røise (Oslo) for assistance with the experiments, and Kenneth Ruud (Oslo) for help with the DALTON program. We are grateful to Mark Brönstrup, Dr. Detlef Schröder, and Prof. Helmut Schwarz (Berlin) for generously sharing their results with us prior to publication.

References

[1] G. Hvistendahl, D.H. Williams, J. Chem. Soc. Perkin Trans. 2 (1975) 881.
[2] G. Hvistendahl, E. Uggerud, Org. Mass Spectrom. 20 (1985) 541.
[3] G. Hvistendahl, E. Uggerud, Org. Mass Spectrom. 26 (1991) 67.
[4] J.R. Gilbert, P.A.M. von Koppen, W.T. Huntress, M.T. Bowers, Chem. Phys. Lett. 82 (1981) 455.
[5] M.T. Bowers, W.J. Chesnavich, W.T. Huntress, Int. J. Mass Spectrom. Ion Phys. 12 (1973) 357.
[6] N.W. Cole, G.J. Rickard, J.R. Christie, P.J. Derrick, Org. Mass Spectrom. 14 (1979) 337.
[7] W.T. Huntress Jr., M.T. Bowers, Int. J. Mass Spectrom. Ion Phys. 12 (1973) 1.
[8] J.H. Jensen, K. Morokuma, M.S. Gordon, J. Chem. Phys. 100 (1994) 1981.
[9] R.H. Nobes, L. Radom, Org. Mass Spectrom. 17 (1982) 340.
[10] R. Nobes, L. Radom, Chem. Phys. 74 (1983) 163.
[11] E.L. Øiestad, Å.M.L. Øiestad, H. Skaane, K. Ruud, T. Helgaker, E. Uggerud, T. Vulpius, Eur. Mass. Spectrom. 1 (1995) 121.
[12] S.M. Bråten, T. Helgaker, E. Uggerud, T. Vulpius, Org. Mass Spectrom. 28 (1993) 1262.
[13] D. Schröder, F. Grandinetti, J. Hrusák, H. Schwarz, Phys. Chem. 96 (1992) 4841.
[14] Å.M.L. Øiestad, E. Uggerud, Int. J. Mass Spectrom. Ion Processes 167/168 (1997) 117.
[15] D. Suárez, T.L. Sordo, J. Phys. Chem. 101 (1997) 1561.
[16] T.G. Lee, M.S. Kim, S.C. Park, J. Chem. Phys. 104 (1996) 5472.
[17] T.G. Lee, S.C. Park, M.S. Kim, J. Chem. Phys. 104 (1996) 4517.
[18] T.G. Lee, Y.M. Rhee, M.S. Kim, S.C. Park, Chem. Phys. Lett. 264 (1997) 303.

[19] E.L. Øiestad, E. Uggerud, Int. J. Mass Spectrom. Ion Processes 165/166 (1997) 39.

[20] E. Uggerud, Eur. Mass. Spectrom. 3 (1997) 403.

[21] J.H. Beynon, R.G. Cooks, Res. Dev. 22 (1971) 26.

[22] M.J. Frisch, G.W. Trucks, H.B. Schlegel, P.M.W. Gill, B.G. Johnson, M.A. Robb, J.R. Cheeseman, T.A. Keith, G.A. Petersson, J.A. Montgomery, K. Raghavachari, M.A. Al-Laham, V.G. Zakrzewski, J.V. Ortiz, J.B. Foresman, C.Y. Peng, P.A. Ayala, M.W. Wong, J.L. Andres, E.S. Replogle, R. Gomperts, R.L. Martin, D.J. Fox, J.S. Binkley, D.J. Defrees, J. Baker, J.P. Stewart, M. Head-Gordon, C. Gonzalez, J.A. Pople, GAUSSIAN 94, Revision D.3, Gaussian, Inc., Pittsburgh, PA, 1995.

[23] T. Helgaker, H.J.Aa. Jensen, P. Jørgensen, J. Olsen, K. Ruud, H. Ågren, T. Andersen, K.L. Bak, V. Bakken, O. Christiansen, P. Dahle, E.K. Dalskov, T. Enevoldsen, B. Fernandez, H. Heiberg, H. Hettema, D. Jonsson, S. Kirpekar, R. Kobayashi, H. Koch, K.V. Mikkelsen, P. Norman, M.J. Packer, T. Saue, P.R. Taylor, O. Vahtras, DALTON, An electronic structure program, Release 1.0, 1997.

[24] C.C.J. Roothan, Rev. Mod. Phys. 23 (1951) 69.

[25] C. Möller, M.S. Plesset, Phys. Rev. 46 (1934) 618.

[26] J.A. Pople, A.P. Scott, M.W. Wong, L. Radom, Israel J. Chem. 98 (1993) 1293.

[27] L.A. Curtiss, K. Raghavachari, G.W. Trucks, J.A. Pople, J. Chem. Phys. 94 (1991) 7221.

[28] F. Angelelli, M. Aschi, F. Cacace, F. Pepi, G.J. de Petris, Phys. Chem. 99 (1995) 6551.

[29] J.E. Del Bene, M.J. Frisch, K. Raghavachari, J.A. Pople, J. Phys. Chem. 86 (1982) 1529.

[30] M.W. Chase Jr., C.A. Davies, J.R. Downey Jr., D.J. Frurip, R.A. McDonald, A.N. Syverud, J. Phys. Chem. Ref. Data 14 (1985) 1.

[31] S.G. Lias, J.E. Bartmess, J.F. Liebman, J.H. Holmes, R.D. Levin, W.G. Mallard, J. Phys. Chem. Ref. Data 17 (1988) 1.

[32] S.T. Gibson, P.J. Greene, J. Berkowitz, J. Chem. Phys. 83 (1985) 4319.

[33] M. Brönstrup, D. Schröder, H. Schwarz, personal communication.

[34] J. Hu, B.T. Hill, R.R. Squires, J. Am. Chem. Soc. 119 (1997) 11699.

[35] K. Ishiguro, M. Ozaki, N. Sekine, Y. Sawaki, J. Am. Chem. Soc. 119 (1997) 3625.

[36] G.A. Janaway, M. Zhong, G.G. Gatev, M.L. Chabinyc, J. Brauman, J. Am. Chem. Soc. 119 (1997) 11697.

[37] M. Aschi, J.N. Harvey, C.A. Schalley, D. Schröder, H. Schwarz, J. Chem. Soc., Chem. Commun. (1998) 531.

[38] H. Ågren, O. Vahtras, B. Minaev, Adv. Quant. Chem. 27 (1996) 71.

[39] J.N. Harvey, M. Aschi, H. Schwarz, W. Koch, Theor. Chem. Acc. Adv. 99 (1998) 95.